



Megaron

<https://megaron.yildiz.edu.tr> - <https://megaronjournal.com>
DOI: <https://doi.org/10.14744/megaron.2025.08684>

M G A R O N

Article

Effects of absorption and scattering values of liquids on global illumination

Ayhan MUCUR^{*}, Togan TONG^{*}

Department of Architecture, Yıldız Technical University, Istanbul, Türkiye

ARTICLE INFO

Article history

Received: 25 December 2024

Revised: 01 June 2025

Accepted: 02 June 2025

Key words:

Absorption; global illumination;
light transport; scattering.

ABSTRACT

In Global Illumination, calculating absorption and scattering values of transparent or semi-transparent materials is one of the most difficult phenomena. Absorption and scattering values affect indirect illumination. This phenomenon is often overlooked in realistic image processing software. When an absorption or scattering coefficient is not input for transparent or semi-transparent materials, the global illumination values do not change. In this study, an experiment was planned to see the effects of absorption and scattering values of liquids on spherical illumination. In the experiment, different liquids were placed in a 55 cm Cornell box, and the illuminance values on the surfaces of the Cornell box were measured for each liquid. The same scene was created with digital image synthesis software. Afterward, the luminance values in the real model and the virtual image were compared. This study proposes adding an absorption and scattering parameter to realistic image synthesis software for transparent and semi-transparent materials. This parameter was prepared with the Open Shading Language (OSL) developed by Sony Imageworks. In this way, the luminance values of the Cornell box in real and digital images are very close to each other.

Cite this article as: Mucur, A. & Tong, T. (2025). Effects of absorption and scattering values of liquids on global illumination. Megaron, 20(2):203–221.

INTRODUCTION

Realistic image synthesis is the process of creating images that are indistinguishable from real photographs using computational methods and advanced techniques. Realistic image synthesis has important applications in many fields such as the film and video industry, virtual (VR) and augmented reality (AR), architecture and urban planning, industrial design, educational simulations, and medical imaging systems. Realistic image synthesis plays an important role in architecture and is not limited to visualization. Beyond determining how a building will look,

it is an efficient tool for building information modeling, building physics, and materials analysis. By simulating the interaction of materials with light, this technology is used to measure their physical properties such as reflectivity, transmittance, and refraction. In addition, when integrated with virtual and augmented reality (VR - AR) technologies, realistic image synthesis has the potential for high-level interaction in the fields of architecture and design. As can be seen, the techniques used in realistic image synthesis, when used correctly and effectively, contribute to the improvement of projects both aesthetically and functionally.

*Corresponding author

*E-mail address: ayhan.mucur@gmail.com



Published by Yıldız Technical University, İstanbul, Türkiye

This is an open access article under the CC BY-NC license (<http://creativecommons.org/licenses/by-nc/4.0/>).

The main goal of realistic image synthesis is to simulate the natural behavior of light and improve the visual fidelity of objects and scenes. Direct illumination, indirect illumination, reflection and refraction, shadows, caustic effects, and global illumination are the basic principles for modeling the behavior of light. Algorithms used to model these principles include ray tracing, radiosity, photon mapping, and path tracing. All these algorithms are different methods for calculating global illumination. Each method, which samples the behavior of light, has advantages and disadvantages over the others. Ray tracing is a point sampling technique that traces infinitesimal light beams through a model (Whitted, 1980). Basic ray tracing, which started in 1980, is based on the principle of tracing light rays from the observer to the light sources. This approach deals only with mirror reflections, refractions, and direct illumination and cannot account for effects such as depth of field, motion blur, caustic, and bright reflections. Radiosity was developed to calculate indirect lighting effects (Cohen & Wallace, 1993). This technique is based on the idea that each surface on the stage can both receive light and act as a light source. It was developed as an alternative to light tracing methods, where the balance of light exchange between surfaces in the scene is calculated. The propagation algorithm is limited to simulating light effects such as the reflection of light from surfaces and its passage through transparent objects. Propagation is mainly designed to calculate the indirect light transfer between surfaces and how this light is scattered. It is often used in combination with other methods, such as ray tracing, to accurately simulate interactions such as reflection and refraction. The strength of the propagation method comes from its ability to calculate the overall illumination of the scene, indirect lighting effects, and the distribution of light between surfaces. Photon mapping shows very successful results in material and surface conditions where ray tracing and diffusion methods are inadequate (Jensen, 2001). This method is a two-step method used in global illumination calculations. The first stage is to record the scattering of photons from light sources and their interactions with surfaces. The second stage is the light calculations that use this information to produce visually accurate images. Photon mapping is suitable for modeling indirect illumination, caustics, and other complex light interactions. It is especially efficient in simulating transparent and semi-transparent objects compared to methods such as light tracing and diffusion. Path tracing is a powerful, realistic image synthesis method that simulates the complex interactions of light in a scene (Kajiya, 1986). By tracing the progression of light paths through the scene, it is able to model phenomena such as reflection, refraction, shadows, and indirect lighting in a natural way. This method works based on the physical laws of the real world. This makes it easy to create challenging effects such as indirect lighting,

complex reflections, and caustics (bright light patterns caused by the refraction of light). In addition to these basic methods, complementary algorithms such as bidirectional ray tracing, Metropolis light transport, and Monte Carlo ray tracing are also used in conjunction with the basic methods.

In global illumination, the most complex situation to compute is the passage of light through transparent and semi-transparent objects. Light exhibits unique interactions, especially as it passes through liquids, being absorbed and scattered depending on the density and components of the liquid. These interactions affect the appearance of the liquid, its depth of color, and how objects in it appear. Absorption is the partial or complete absorption and retention of the energy of light as it travels through a medium. Liquids absorb certain wavelengths of light, causing the liquid to acquire a distinctive color. Accurately simulating absorption values allows liquids to gain a realistic sense of color and depth. Scattering is the change in direction of light as it travels through a medium. This feature causes the light to spread over a wider area in the liquid, creating a soft lighting effect in the process. Accurate modeling of scattering in a liquid affects the opacity of the liquid and the visibility of objects in it. Accurate calculation of absorption and scattering values ensures that the colors of liquids and the objects in them are seen realistically, which contributes to the overall atmosphere of the scene. Absorption rates, which vary depending on the depth of the liquids, create a perception of depth in the scene. Scattering creates soft lighting effects in and around the liquid and makes the shadows on the liquid surface and on the objects in it appear more realistic. Absorption and scattering determine how clear objects in the liquid appear. This is important for the degree of blur in the liquid and the visibility of details behind objects.

Accurate modeling of the absorption and scattering values of liquids, as part of global illumination algorithms, plays a critical role in producing photorealistic images. This is especially important in scenes involving transparent materials such as water, glass and different liquids to enhance visual realism.

BACKGROUND

Global Illumination

Global Illumination (GI) is a lighting model in computer graphics and rendering technologies that provides a realistic calculation of the light in a scene. GI takes into account not only the light coming directly from the light source but also the light that is reflected between surfaces and objects in the scene and reaches other surfaces indirectly (Angel & Shreiner, 2020). This approach allows for more natural and detailed lighting and shadows to be created in scenes. For example, thanks to GI, light reflected from one surface carries its color to other surfaces, adding

a color-bleeding effect to the scene. Based on the principle of energy conservation, this model is compatible with physically based rendering (PBR) and ensures that the total energy of light remains constant in the scene (Peddie, 2019). GI simulates direct and indirect light calculations with ray tracing and path tracing, while techniques such as radiosity and photon mapping are used to model complex light distribution. In addition, volumetric lighting adds depth to scenes by accounting for the transport of light in participating environments (e.g. fog and smoke). GI is indispensable for providing lifelike and dynamic lighting in areas such as film, animation, architectural visualization, and modern game development.

Basic Radiometric Quantities

Radiometry is the field that deals with the entire electromagnetic spectrum, including visible light, and studies the measurement of radiation. In this context, three fundamental quantities are considered: flux, irradiance, and radiance (Kurachi, 2007).

- Radiant Flux (Φ) is the total electromagnetic energy emitted from a source in a given time interval. Its unit is expressed in Watts (W) (Table 1).
- Irradiance (E) is the energy flux falling on a surface. It is defined as the amount of energy incident on a surface area and is expressed in watts/square meter (W/m^2). It is often used when analyzing sunlight or other light sources (Table 1).
- Radiance (L) is the flux of energy emitted or reflected from a unit area in a given direction. This quantity provides information about both the direction of light and the amount of light leaving the source. It is expressed in watts/(square meter-steradian) [$\text{W}/(\text{m}^2\text{-sr})$] (Table 1).

Table 1. Radiometric quantities and expressions

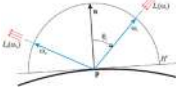
Reference	Quantity	Formula Expression
	Radiant Flux (Φ)	$\Phi = \frac{dQ}{dt}$
	Irradiance (E)	$E(p) = \frac{d\Phi(p)}{dA}$
	Radiance (L)	$L(p, \omega) = \frac{d^2\Phi(p, \omega)}{dA d\omega \cos \theta}$ $= \frac{dE(p, \omega)}{d\omega \cos \theta}$

Table 2. Radiometric and photometric units

Quantity	Radiometric Unit	Photometric Unit
Radiant Flux (Φ)	Watt (W)	Lumen (lm)
Irradiance (E)	Watt per square meter (W/m^2)	Lux (lx)
Radiance (L)	Watt per square meter per steradian ($\text{W}/(\text{m}^2\text{-sr})$)	Candela per square meter (cd/m^2)
Radiant Intensity (I)	Watt per steradian (W/sr)	Candela (cd)

Radiometric units cover the entire electromagnetic spectrum, while photometric units are organized according to the visible light spectrum, which only the human eye can detect. Therefore, radiometric and photometric units differ from each other (Table 2).

BRDF-Based Lighting Models

BRDF (Bidirectional Reflectance Distribution Function) is a mathematical function that defines the angle and intensity at which light coming to a surface is reflected from this surface. It determines the scattering of light in different directions by reflecting from the point where it hits the surface and thus analyzes the optical properties of the surface (Zhou, 2023). BRDF models the interaction of light with the surface, simulating the physical properties of the material such as matte, glossy, metallic or translucent. This function is used in computer graphics and rendering processes to obtain realistic visualizations. It helps calculate both the direct and indirect lighting. BRDF-based lighting models increase the realism of reflections in scenes by also taking into account the interactions of light with the texture and microstructures of the surface (Guarnera et al., 2016).

The image of objects in the real world is formed when ambient light is reflected from the surface of the object and reaches our eyes. BRDF is a function that describes the relationship between light incident on a surface and reflected light (Figure 1). Its mathematical expression is as follows:

$$f_r(p, \omega_i, \omega_o) = \frac{dL_o(p, \omega_o)}{dE_i(p, \omega_i)} = \frac{dL_o(p, \omega_o)}{L_i(p, \omega_i) \cos \theta_i d\omega_i}$$

In this equation,

- $f_r(p, \omega_i, \omega_o)$ represents the BRDF
- p is a point on the surface
- ω_i is incoming light directional
- ω_o is the direction of the observer or reflected light
- $dL_o(p, \omega_o)$ is the differential reflected radiance of the surface in the direction ω_o
- $dE_i(p, \omega_i)$ is the differential illuminance of the surface from the incoming light direction ω_i
- θ is the angle between the incoming light direction ω_i and the surface normal at the shading point p .

Integrating over the entire semi-spherical surface:

$$L_o(p, \omega_o) = \int_{\Omega} f_r(p, \omega_i, \omega_o) L_i(p, \omega_i) \cos \theta_i d\omega_i$$

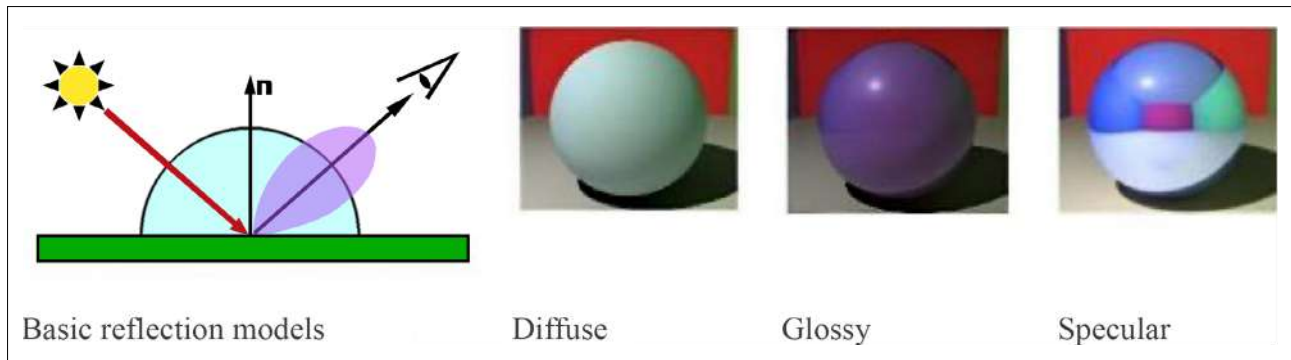


Figure 1. Basic reflection models for incident light (Goral et al., 1984).

In general, BRDF describes the distribution of outgoing light after it reflects from a point on the object's surface with the direction of the incoming light. In computer graphics, the BRDF is represented as a three-component RGB vector. BRDF has basic properties such as reversibility, energy conservation, and linearity.

The reversibility of the BRDF is based on the Helmholtz Reciprocity Principle, which states that changing the incident and reflected light will not change the BRDF value:

$$L_0(p, \omega_i, \omega_o) = L_0(p, \omega_o, \omega_i)$$

BRDF is also subject to the principle of energy conservation. The energy conservation equation is as follows (Q represents the corresponding energy):

$$Q_{incoming} = Q_{reflected} + Q_{absorb} + Q_{transmitted}$$

Therefore, it can be concluded that:

$$Q_{reflected} \leq Q_{incoming}$$

Therefore, the BRDF must satisfy the following integral inequality for the energy conservation property:

$$\forall \omega_i, \int_{\Omega} f_r(p, \omega_i, \omega_o) \cos \theta_i d\omega_i \leq 1$$

The linearity property of BRDF requires multiple BRDF calculations for the correct reflection description. The total reflected radiance of a point on a surface can be simply represented as the sum of the individual BRDF reflected radiances. For example, bright diffuse reflectance can be obtained by calculating multiple BRDFs.

To make BRDF data easier to process and more efficient, the researchers translated them into numerical models. These models were categorized as empirical and physically based. In addition, data-driven models were developed to directly obtain measured BRDF data and use it in the processing process.

Empirical Models

Empirical models are generally focused on the calculation of reflected light. They produce simple formulas for fast calculations on this subject. Empirical models include parameters based on observation of the behavior of light and provide results close to physical reality. However, they

may not fully meet the laws of physics such as reversibility and conservation of energy.

In 1975, Bui Tuong Phong (Phong, 1975) introduced the Phong Reflection Model to simulate specular reflections. Considered one of the earliest BRDF models, it described the light reflected by a point on a surface towards an observer as the sum of various light intensities. The Phong Reflectance Model is one of the most basic and common reflectance distribution functions used to model how surfaces reflect light and provides a simple yet effective approach to making surfaces appear matte or shiny. For this reason, it is still used today as a basic reference in many computer graphics applications.

The Phong model describes the behavior of light on a surface with two main components. Diffuse accounts for the dispersion of light on the surface, and specular accounts for the reflection of light back to the observer. Thus, the Phong BRDF combines these two components to calculate the reflection behavior of a surface. However, the Phong model fails to simulate more complex surface properties and micro-surface details.

In 1977, Jim Blinn (Blinn, 1977) developed the Blinn-Phong reflection model as an improvement to the Phong model. The Blinn-Phong model simplifies some of the calculations of specular reflections in the Phong model and provides a more efficient computational process while providing similar visual results. For this reason, it has become widely used in computer graphics. Although the Phong model uses the angle between the ideal reflection vector and the view vector to calculate the specular component, the Blinn-Phong model uses a different vector called the half-vector. The half-vector represents the direction halfway between the light source vector and the line-of-sight vector, so the calculation is performed with this half-vector instead of the ideal reflection vector. This method is particularly computationally efficient and provides a more stable result.

The Blinn-Phong model produces more realistic specular highlights, especially on surfaces with high specular exponential values. Highlights appear more diffuse or more focused depending on the smoothness of the surface and

the light source. This increases realism by making surfaces look more natural. In addition, the half-vector calculation reduces visual errors due to changes in the angle between the light source and the observer. However, the Blinn-Phong model, like the Phong model, does not take into account the orientation of the observer relative to the surface. This can lead to inaccurate reflections at some angles.

In 1992, Ward (Ward, 1992) proposed the Ward BRDF model, an empirical model developed by measuring and fitting reflection data of objects. This model was an important step forward, especially for photorealistic imaging and the simulation of light reflection properties. In particular, he aimed to more accurately model the reflection properties of metallic surfaces. Ward's BRDF model takes into account the effects of surface roughness and micro-geometric properties on reflections in areas where traditional Lambertian surfaces are inadequate in reflection modeling. Based on the assumption that the micro-roughnesses on the surface are randomly distributed, the Ward BRDF model determines the different reflectance amounts of these roughnesses according to the directions. Therefore, the Ward model more accurately describes the reflection behavior of anisotropic surfaces (i.e., surfaces with different properties in different directions).

However, the original Ward BRDF model has energy loss when light is scattered. In 2006, Arne Dür (Dür, 2006) made some additions to Ward's model and introduced a more accurate and flexible reflection model. The Ward-Dür model ensured that surface reflections conform to the principles of energy conservation. In 2010, Geisler-Moroder and Dür (Geisler-Moroder & Dür, 2010) developed the Ward-Dür BRDF model to conserve energy at all angles. This version of the model addresses the problem of energy conservation by introducing a finite albedo parameter that helps to ensure that the model remains physically plausible at all angles. However, Ward's 1992 BRDF model is considered a revolutionary development, especially for computer graphics and rendering engines.

In 2000, Ashikhmin & Shirley (Ashikhmin & Shirley, 2000) proposed a new BRDF model inspired by the models of Ward (Ward, 1992), Schlick (1994), and Neumann et al., (1999). The Ashikhmin-Shirley model was a new experimental model with many desirable properties, such as energy conservation and reciprocity. It allows anisotropic reflection to create effects such as the striped appearance of brushed metal. The parameters of the model are intuitive and take into account the Fresnel effect, which causes the specular reflection to increase as the angle of incidence decreases. In addition, the diffuse term is not constant, so the diffuse component decreases as the angle of incidence decreases. This model is well suited for Monte Carlo processing techniques.

Physically-Based Models

Physically based models are models that calculate surface reflectance in more detail based on physical principles and produce more accurate results. Because they are physically accurate, they are particularly suitable for realistic rendering and simulations. These models more accurately describe the microstructure of surfaces and the direction of light reflection. Physically based BRDF models are based on physics concepts such as energy conservation and Helmholtz reciprocity.

In 1967, Torrance & Sparrow (1967) used radiation and microfacet theory to produce a rough surface specular reflection model. In 1981, Cook & Torrance (1981) introduced the Cook-Torrance model, an improved version of the Torrance-Sparrow model. The Cook-Torrance model is based on the microsurface theory. According to this theory, the irregular structure of the surface consists of tiny bends and ridges at the micro level and light interacts with these micro surfaces and reflects at different angles depending on the degree of roughness of the surface. This reflection model takes into account not only the reflection properties of the surface, but also the effects of roughness, shadowing, and light refraction.

The Cook-Torrance model is a microfacet model widely used in computer graphics. It is used to simulate the appearance of metal and glass materials and has many advantages, notably the Fresnel effect. In this model, the Fresnel effect, the reflection of light at tangential angles from surfaces, is more accurately calculated, and the anisotropic reflection used to achieve the appearance of brushed metal is also obtained. In addition, the Cook-Torrance model is used to model a wide range of materials, from dull to shiny surfaces.

In 1991, He et al., (1991) published a paper proposing a more complex and purely physical BRDF model based on wave optics. This model takes into account the polarization of smaller scattering angles of light, diffraction, interference, surface conductivity, and roughness, and can simulate more optical phenomena than microfacet models. However, the computational cost is much higher.

The Oren-Nayar model was introduced by Oren & Nayar (1994) in 1994. This model was developed for rough surfaces and establishes a relationship between surface roughness and reflection pattern. One of the main advantages of the Oren-Nayar model is that it simulates the surface roughness of real objects to a certain extent, giving them a more textured appearance. However, it may not be suitable for real-time applications as the computation times are too long.

Data-Driven Models

Data-driven models are a type of general model that provides a way to quantify anisotropic BRDFs based on measured

data. These save a large set of BRDF materials as high-dimensional vectors and then use dimension reduction to compute a low-dimensional model from this data. This allows a lookup table-based approach to directly find processing results and saves a lot of real-time computation. Matusik et al., (2003) described in their 2003 paper how they implemented a series of studies and obtained a data-driven reflectance model. In addition, many laboratories have used a variety of tools to measure reflectance data of various real-world materials under different light angles and observation angles and recorded them in public databases such as the MERL BRDF Database.

Since data-driven models are based on measurements of real-world materials, the resulting renders are very realistic, and this is one of the main advantages of these models. However, a major drawback is the lack of parameters for adjusting effects, so it is not possible to manipulate the data to achieve the desired results. In addition, data collection for some extreme angles is difficult due to instrument limitations. These models also require large amounts of data and are computationally expensive, making them less suitable for real-time applications such as video games, but suitable for offline renders such as movies. They can also be used in graphics research to evaluate the realism of other BRDF models.

Participating Media-Based Lighting Models

Participating media-based lighting models are lighting models that simulate how light interacts not only with surfaces but also with particles within a medium. These media can be transparent or translucent substances such as air, fog, smoke, water. Participating environments take into account the absorption, scattering and redirection of light, resulting in a more realistic and immersive visual experience in scenes (Cerezo et al., 2005).

Participating media are volumes filled with particles that affect the light passing through them by scattering or absorption. This term refers to media that actively participate in the transmission of light. In computer graphics, low-density media such as water, fog, steam, and air, in addition to solid surfaces, are also important for modeling their interactions with light. The composition and particle density of a medium determine the behavior of light in the medium. In homogeneous media (e.g., air or water), the density is constant, while in heterogeneous media (e.g., clouds or steam), the density is variable. Some dense materials, such as skin or candle wax, exhibit high levels of light scattering, and such interactions form the basis of diffuse surface shading models. As a result, all media scatter or absorb light to some extent, depending on their density and composition (Deng et al., 2020).

In recent years, various algorithms have been introduced to handle participatory media, such as many light-based

methods (virtual ray lights, VRL) (Novák et al., 2012), various extensions to photon mapping resulting in unified points, rays and paths (UPBP) (Křivánek et al., 2014), Monte Carlo-based methods (Herholz et al., 2019) and point-based methods (Wang & Holzschuch, 2017). All these methods have greatly improved the simulation of participating media.

Features of Participating Media

In a participating medium, three different phenomena affect the amount of radiation emitted along the beam (Siegel & Howell, 1992).

- **Absorption:** The medium absorbs some of the light, and the light energy is converted into heat or other energy. The intensity of light absorbed determines the degree of opacity of the medium.
- **Scattering:** Light changes direction when it hits particles in the medium. This process scatters some of the light in other directions. In Single Scattering, light is scattered only once and then either hits the observer or another surface. In Multiple Scattering, light is scattered more than once in many directions. This is more pronounced in dense environments.
- **Light Extinction:** Light loses intensity due to both absorption and scattering.

Participating media-based lighting models are usually based on the Radiative Transfer Equation (RTE). This equation mathematically describes the absorption, scattering, and propagation of light in a medium (Table 3):

$$L(x, \omega) = L_e(x, \omega) + \int_V \sigma_s(x, \omega') \cdot L(x, \omega') \cdot p(\omega', \omega) d\omega'$$

In this equation,

- $L(x, \omega)$ is the light intensity at a given point (x) and direction (ω).
- $L_e(x, \omega)$ is the light emitted from a light source.
- $\sigma_s(x, \omega')$ is the scattering coefficient.
- $p(\omega', \omega)$ is the phase function (determines which direction the light is scattered).

Table 3. Features and units used in participating media (Akenine-Möller et al., 2018)

Symbol	Feature	Unit
σ_a	Absorption coefficient	m^{-1}
σ_s	Scattering coefficient	m^{-1}
σ_t	Extinction coefficient	m^{-1}
ρ	Albedo	unitless
p	Phase function	sr^{-1}

Types of Participating Media-Based Lighting Models

- **Volumetric Lighting:** A lighting method in computer graphics and visualization that simulates how light propagates, absorbs, and scatters through a medium. It is used to model the interactions of light with participating media such as smoke, fog, vapor, or water instead of solid surfaces. This technique is particularly important for adding depth, atmosphere, and dramatic visualization to scenes (Novák et al., 2018).
- **Ray Marching:** Although it works on a similar principle to ray tracing, ray marching calculates the density of the medium or its distance from the surface at each step the light travels, which is a great advantage, especially for complex volumetric media.
- **Single Scattering:** This model simulates situations where light is scattered only once. It is less complex and gives fast results in low-density environments (e.g. light fog). However, it does not provide realism in dense environments such as multiple scattering (Jönsson et al., 2014; Yan et al., 2013).
- **Multiple Scattering:** Simulates the complex interactions that occur when light is scattered more than once. It can produce more realistic results for environments such as dense fog, smoke, or water. Computational cost is high, but the results are highly detailed (Jönsson et al., 2014; Yan et al., 2013).
- **Subsurface Scattering:** Simulates light penetrating translucent materials (such as skin, wax, milk), propagating through them and then exiting. This model is especially used for realistic visualization of organic materials such as skin (Dutré et al., 2006; Kurachi, 2007).

Comparison of BRDF and Participating Media-Based Lighting Models

These models are the two main approaches used to model the interaction of light with different physical media. BRDF-based models deal with the interactions of light with surfaces while participating media-based models simulate how light propagates, absorbs, and scatters within a volume (participating media) (Table 4).

BRDF (Bidirectional Reflectance Distribution Function) is a model that describes the light reflection of surfaces. It calculates the reflection of light from a surface depending on the incoming and outgoing light angles. It is often used for opaque surfaces and simple lighting situations. BRDF models are fast, so they are common in real-time rendering engines, but focus only on surface effects.

Participating media-based models simulate the propagation, scattering, and absorption of light in a medium. These models are ideal for handling volumetric effects such as fog, smoke, or water. Participating ambient models focus on physical accuracy but are computationally expensive and are often favored in cinematic rendering engines.

As a result, BRDF is simpler and faster, suitable for surface reflections. Participating environment models, on the other hand, are more complex but are required for effects that aim for volumetric and physical accuracy. The two are often used together to optimize both surface and volumetric lighting effects.

METHOD

In this study, an experiment was planned to determine the effects of absorption and scattering values of liquids on global illumination. In this experiment, a glass filled with different liquids was placed in a 55cm Cornell box and the luminance values on the surfaces of the Cornell box were measured for each different liquid. The same scene was created digitally with V-Ray 6 and Corona software for image synthesis. As a result, the surface luminance values of the real model and the virtual image were compared.

- **Color Contrast:** The colors red and green are opposite each other in the color spectrum. This contrast makes it easier to observe the reflection and propagation of light on different surfaces. Thus, the behavior of light on different colors can be analyzed more clearly.
- **Light Reflection and Diffusion:** Different colors reflect and diffuse light in different ways. Strong colors such as

Table 4. Comparison of BRDF and participating media-based models

Feature	BRDF-Based Models	Participating Media-Based Models
Focus	Surface-Oriented	Volume-Oriented
Type of Interaction	Reflection, Refraction	Absorption, Scattering, Multiple Scattering
Physical Theories	Fresnel Reflection, Micro-face Distribution, Conservation of Energy	Radiative Transfer Equation
Physical Accuracy	High Accuracy for Surface Materials High Accuracy in Volumetric Environments	
Calculation Cost	Lower	Higher
Areas of Usage	Metal, Glass, Plastic Surfaces	Fog, Smoke, Liquid, Atmospheric Effects

red and green make the behavior of light on these surfaces apparent. In this way, the reflection and propagation properties of light can be studied in more detail.

- **Realism and Accuracy:** The use of red and green colors is used to test the accuracy of calculations made to create realistic scenes in computer graphics and visual effects. These colors are ideal for testing light and shadow interactions and how the human eye perceives these interactions.
- **Psychological Impact:** The colors red and green are easily distinguishable to the human eye. This allows observers to analyze light and color interactions more easily.

The experiment was conducted with a 55 cm Cornell box, a surface-mounted luminaire and a measuring device (Figure 2). The interior surfaces of a 55 cm box were painted with RAL code-defined colors (Table 5) (Figure 3).

The equivalents of the three colors on the experiment box surfaces in all other color systems have been calculated (Table 6). These values will be the reference in the virtual experiment to be conducted later.

The luminaire is a surface-mounted model used for indoor lighting (Table 7). Luminaire, supplied by İkizler Lighting, has been tested again in the company's laboratory. The technical data of the products manufactured in industrial design are very close to each other. However, due to production conditions, the values are not exactly the same. All technical features of the luminaire have been re-measured in order to simulate the virtual scene very close to reality. In addition, the IES Map has been prepared to be used in the 3D scene.



Figure 2. Experiment box, luminaire, spectroradiometer, and liquids.

Table 5. RAL codes for the Cornell box

Surface	RAL Codes
Red Surface	RAL 3020
Green Surface	RAL 6001
White Surface	RAL 9003

Konica Minolta CS-2000 Spectroradiometer was used for the measurements (Figure 4).

In the Cornell Box, the luminance values on the box surfaces were measured for an empty glass and 8 different liquids. The value changes in different liquids were compared in tables. In this experiment, an empty glass, water, milk, olive oil, white wine, red wine, beer, honey, and grape vinegar were used (Figure 5). Measurement values are (cd/m^2).

For each liquid, luminance values were measured at 16 different points on the Cornell box surface (Figure 6). In addition, an identification number is defined for the points defined on the colored surfaces (Table 8).

In this experiment, the change in luminance values of points determined on the Cornell box surfaces under the influence of different liquids was investigated. The luminance value at each point is the sum of the direct light, reflected light, and indirect light reaching after being absorbed by the liquid (Figure 7).

The luminance values of three different surfaces in the Cornell Box were measured. Each surface was divided into three equal parts horizontally and vertically after leaving a 2 cm gap from the edges. Thus, 4 axes intersecting each other horizontally and vertically were formed. The intersection points of these axes are the 16 points to be measured. The luminaire located in the middle of the upper surface of the Cornell box emits light in all directions at 180 degrees. In this case, each point on the surface to be measured is at a different position and angle from the light source. In this sense, measuring from 16 different points for each surface is an important factor in understanding the distribution and reflection of light (Table 8).

Experiment Results

In the measurements, it is seen that the red and green surface values are close to each other (Table 9; Table 10; Figure 8; Figure 9). However, it was determined that the white surface values are different from the red and green values (Table 11) (Figure 10). While the red and green surfaces have the same angle and position as the light source, the angle and position of the white surface are different. The luminance value on the surfaces is the sum of four different light values (Figure 7). These are the direct light coming from the luminaire, the indirect light coming by bouncing off other surfaces, the indirect light coming by reflecting off the glass surface, and the indirect light coming after being absorbed in the glass. In this case, the only element that will affect the values in measurements made with different liquids is the liquid in the glass. The values are affected by the different color and absorption coefficients of these liquids. The purpose of this study is to determine whether these experimental findings made with a real model give the same results in software that performs realistic image synthesis.



Figure 3. Experiment box and RAL codes.

Table 6. Color code equivalents in other color systems

RAL 6001				
RGB	54, 103, 53	CSS	rgb (54, 103, 53);	
HSL	119, 32, 31	CSS	hsl (119, 32%, 31%);	
HSB	119, 49, 40	Hex	#366735	
CMYK	80, 30, 100, 10	Websafe	#336633	
RAL 3020				
RGB	187, 30, 16	CSS	rgb (187, 30, 16);	
HSL	5, 84, 40	CSS	hsl (5, 84%, 40%);	
HSB	5, 91, 73	Hex	#bb1e10	
CMYK	0, 100, 100, 10	Websafe	#cc3300	
RAL 9003				
RGB	236, 236, 231	CSS	rgb (236, 236, 231);	
HSL	60, 12, 92	CSS	hsl (60, 12%, 92%);	
HSB	60, 2, 93	Hex	#ecece7	
CMYK	0, 0, 0, 0	Websafe	#ffffff	

Table 7. Technical Specifications of the Luminaire

Luminaire Photometric Test Report

Test: U:224.20V I:0.0873A P:18,674W PF: 0.9544 Freq:50.03Hz UTHDi:0.00%

Lamp Flux:983,472x1 lm

Name	Canvas-T	Type	Su	Weight	0.6 kg
Spec.	4000K	Dim.	175x175x115mm	Serial No.	05250.22.40.022.N000
Mfr.	İkizler Lighting	Sur.		Shielding Angle	
Data of Lamp		Photometric Data	Eff: 52,66 lm/W		
Model	Led	Imax (cd)	338.1	S/MH (C0 / 180)	1.25
Nominal Power (W)	18.67	LOR (%)	100.0	S/MH (C90 / 270)	1.26
Rated Voltage (V)	220	Total Flux (lm)	983.47	η UP, DN (C0 - 180)	0.9 – 49.2
Nominal Flux (lm)	983,472	CIE Class	Direct	η UP, DN (C180 - 360)	0.6 – 49.2
Lamps Inside	1	η up (%)	1.6	CIBSE SHR NOM	1.25
Test Voltage (V)	220	η down (%)	98.4	CIBSE SHR MAX	1.35

Virtual Scene Experiment

The experiment, the technical details of which are described above, was simulated in 3D environment. Cornell box, luminaire, and glass were modeled with the same dimensions and material properties were defined. The luminaire used was re-measured in the manufacturer's laboratory and an IES map was taken by these values. The RAL color codes of the surfaces were converted to RGB values and this value was processed into the material properties. V-ray 6.0 and Corona 11 were used as image-processing software. Surface luminance values were measured as (cd/m²) with the VrayLightingAnalysis render element module in V-Ray software. Since Corona software does not have a Light Analysis module, indirect illuminance values on the surfaces were measured with the Indirect Light render element module.



Figure 4. CS-2000 Spectroradiometer.

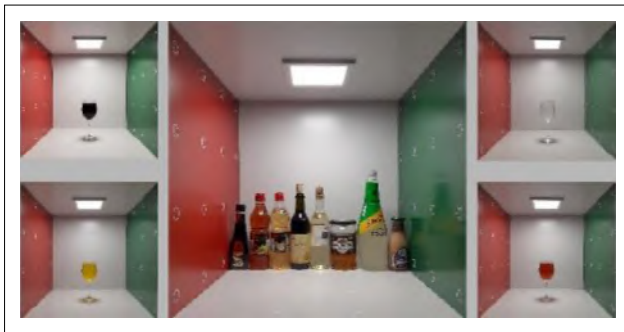


Figure 5. Empty glass and 8 different liquids.



Figure 6. Experiment box and measuring points.

Virtual Scene Material Properties

The materials of the red, green, and white surfaces are defined by Diffuse - Roughness, Reflection - Glossiness, and Fresnel Reflection parameters. V-RayIES light was used for the light value in the luminaire illumination. The material properties of the glass and all liquids are defined by the parameters Diffuse - Roughness, Reflection - Glossiness, Fresnel Reflection, Refraction - Glossiness - IOR, and Translucency - Fog Color - Depth(cm).

Table 8. Measurement points inside the Cornell box

Surface Measurement Points	
Red Surface	L01, L02, L03, L04, L05, L06, L07, L08, L09, L10, L11, L12, L13, L14, L15, L16
Green Surface	L17, L18, L19, L20, L21, L22, L23, L24, L25, L26, L27, L28, L29, L30, L31, L32
White Surface	L33, L34, L35, L36, L37, L38, L39, L40, L41, L42, L43, L44, L45, L46, L47, L48

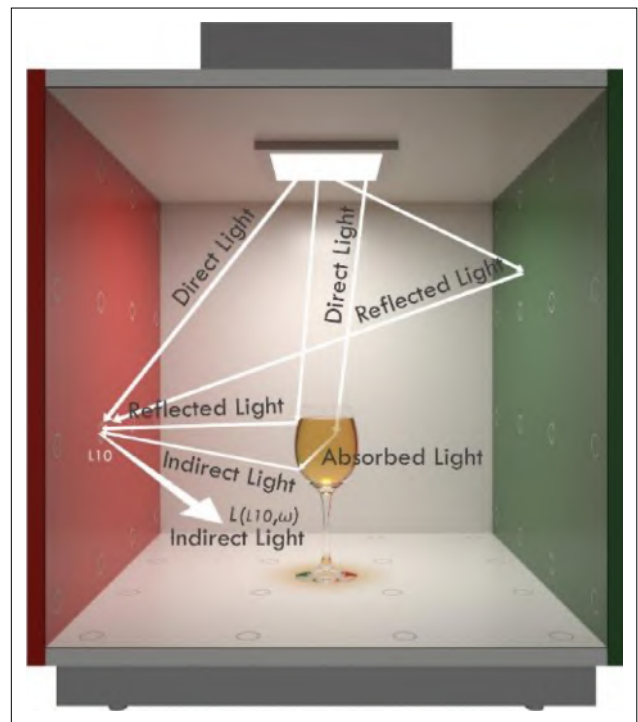


Figure 7. Example light scheme at point L10.

Virtual Experiment Results

Realistic renders of the Cornell box and liquids created with V-ray 6 software (Figure 11; Figure 12; Figure 13):

Light analysis renders of the Cornell box and liquids created with V-ray 6 software (Figure 14; Figure 15; Figure 16):

Realistic renders of the Cornell box and liquids created with Corona 11 software (Figure 17; Figure 18; Figure 19):

Indirect light renders of the Cornell box and liquids created with Corona 11 software (Figure 20; Figure 21; Figure 22):

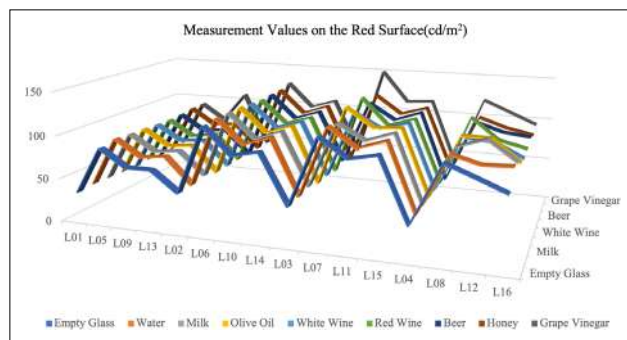
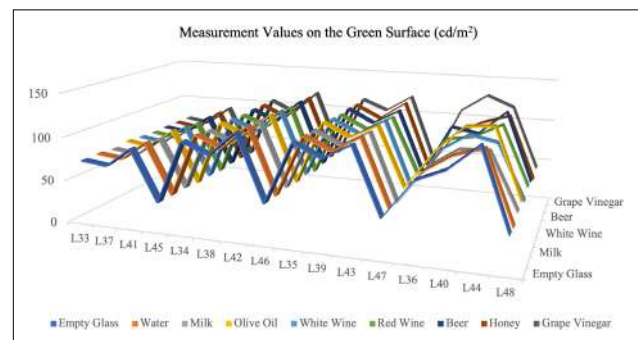
The measurement values taken from the surfaces in the real model experiment do not match the surface measurement values in the images created in V-ray and Corona software. The reason for this is that the software generally does not define an absorption coefficient for liquid materials. Each transparent and semi-transparent material has its own absorption coefficient. Open Shading Language (OSL) was preferred to add this feature to the software. Open Shading

Table 9. Measurement values on the red surface of the Cornell box (cd/m²)

Liquids	L01	L05	L09	L13	L02	L06	L10	L14	L03	L07	L11	L15	L04	L08	L12	L16
Empty Glass	32.68	86.69	66.96	67.11	43.98	121.5	91.86	98.54	42.53	120.1	99.59	106.1	36.35	104.1	91.74	79.04
Water	34.24	90.5	71.48	75.1	44.79	123.8	96.42	107.6	44.39	124.3	103.2	113.8	37.66	105.3	96.67	98.34
Milk	33.39	89.28	70.71	73.92	47.81	123.8	95.97	107.3	46.96	121.1	104.4	115.1	38.54	105.7	115.9	94.22
Olive Oil	32.58	88.97	70.42	73.42	43.54	124	96.55	107	42.33	132.8	111.9	113.8	38.2	110.3	110.1	85.89
White Wine	31.61	87.83	70.23	72.66	43.84	122.9	96.18	105.2	43.3	120.8	104.2	112.9	38.3	100.9	98.3	82.78
Red Wine	33.31	87.49	69.09	73.53	44.31	121.5	94.9	104.2	40.89	132.2	101.5	111.6	37.91	117.7	93.84	86.25
Beer	31.65	88.53	69.91	72.68	42.82	123	95.05	105.4	45.78	120.5	101.9	112.9	34.14	106.3	96.41	92.96
Honey	32.95	90.92	71.45	73.89	43.99	123.7	95.76	106.6	42.35	124.7	103.3	112.8	39.61	105.5	94.99	88.45
Grape Vinegar	34.35	91.49	71.89	108.2	44.37	127.6	97.97	107.8	44.32	149.5	113.1	115.3	37.98	120.9	107.8	94.52

Table 10. Measurement values on the green surface of the Cornell box (cd/m²)

Liquids	L33	L37	L41	L45	L34	L38	L42	L46	L35	L39	L43	L47	L36	L40	L44	L48
Empty Glass	71.8	68.2	91	31.8	104	91.7	119	44	113	99.1	116	42.2	84.4	98.4	126	39.4
Water	72.3	68.4	91	31.5	104	91.7	119	43.7	113	99	117	42.5	84.8	105	115	36.8
Milk	70.7	66.3	88.6	31.5	103	90.8	119	44.5	113	98.3	115	39.7	83	104	105	43.1
Olive Oil	73.4	68.9	91.5	29.5	106	92.5	120	42.4	116	100	116	47.9	91.8	122	125	45.5
White Wine	72.1	67.4	89.8	30.1	104	90.9	119	43.6	113	98	115	40.7	85.8	106	99.6	36.1
Red Wine	71.3	66.4	88.1	28.7	103	90.3	117	39.6	112	96.9	113	48	91.7	96.7	114	44.2
Beer	72.1	67.1	89.9	30.4	104	90.7	119	41.6	114	98.1	115	40.4	100	94.1	122	42
Honey	72.4	66.9	90.1	30.4	104	90.2	118	42.6	113	97.8	119	40.2	85.2	101	111	36.2
Grape Vinegar	72.3	67.6	90.3	29.4	105	91	119	41.1	114	102	122	40.7	108	129	116	42.4

**Figure 8.** Radiance change graph on the red surface.**Figure 9.** Radiance change graph on the green surface.

Language (OSL) was preferred because it works integrated with rendering software such as Arnold, Blender/Cycles, Pixar/Renderman, Chaos/V-ray, Chaos/Corona.

Adding Parameters with Open Shading Language

This work continues in terms of analyzing other realistic image processing software and preparing the code infrastructure of the proposed parameters. Software such as Arnold Renderer and Renderman are being analyzed. In addition, it is planned to add the proposed parameters to the materials with the Open Shading Language (OSL) language developed by Sony ImageWorks.

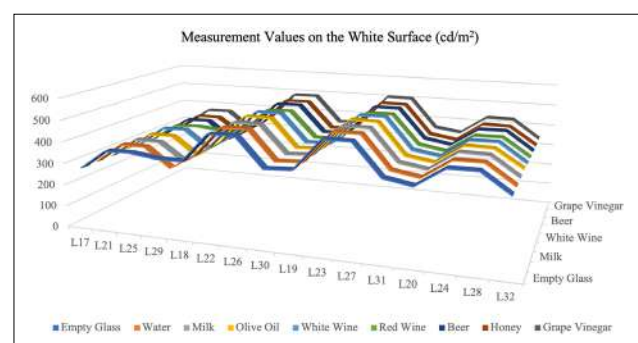
**Figure 10.** Radiance change graph on the white surface.

Table 11. Measurement values on the white surface of the Cornell box (cd/m²)

Liquids	L17	L21	L25	L29	L18	L22	L26	L30	L19	L23	L27	L31	L20	L24	L28	L32
Empty Glass	275	363	366	350	349	480	482	350	356	497	497	357	335	420	421	336
Water	276	365	365	276	351	482	485	351	358	502	501	357	336	423	423	337
Milk	274	362	359	275	353	481	481	354	361	502	501	360	340	427	424	339
Olive Oil	279	361	361	275	354	485	486	353	362	506	502	359	340	425	423	344
White Wine	277	364	368	279	352	483	484	354	357	501	501	358	338	422	424	338
Red Wine	273	355	360	348	347	469	472	349	352	489	490	355	333	416	418	335
Beer	276	360	365	278	350	478	480	352	355	496	495	357	336	420	422	336
Honey	274	359	358	274	347	474	475	348	356	493	492	353	333	420	417	335
Grape Vinegar	282	368	370	280	357	484	485	355	363	503	502	361	344	430	428	341

**Figure 11.** V-ray realistic renders of empty glass, water, and milk.**Figure 12.** V-ray realistic renders of olive oil, white wine, and red wine.

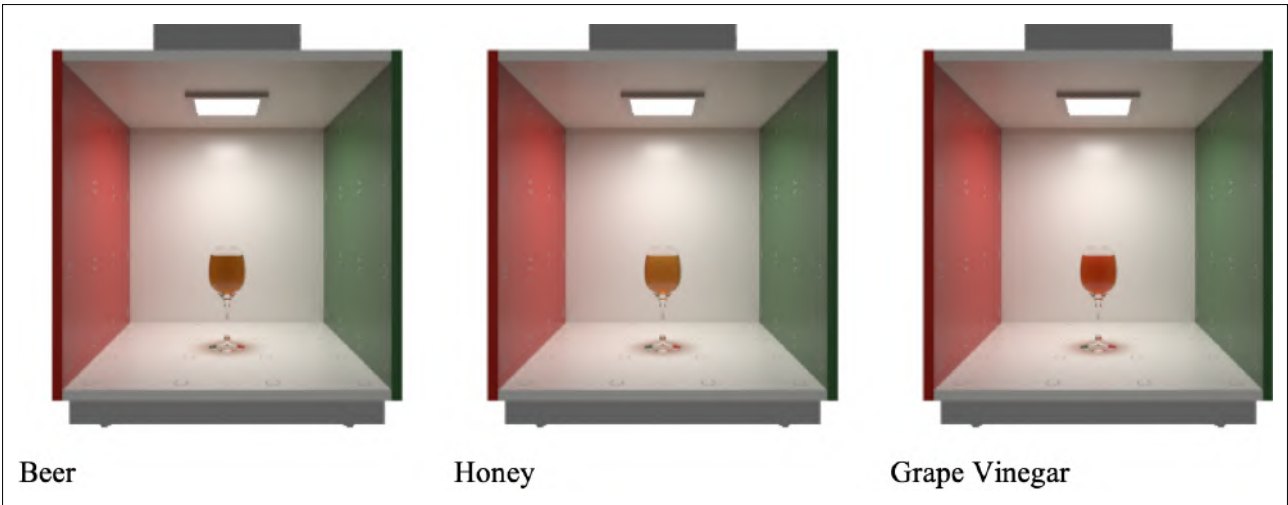


Figure 13. V-ray realistic renders of beer, honey, and grape vinegar.

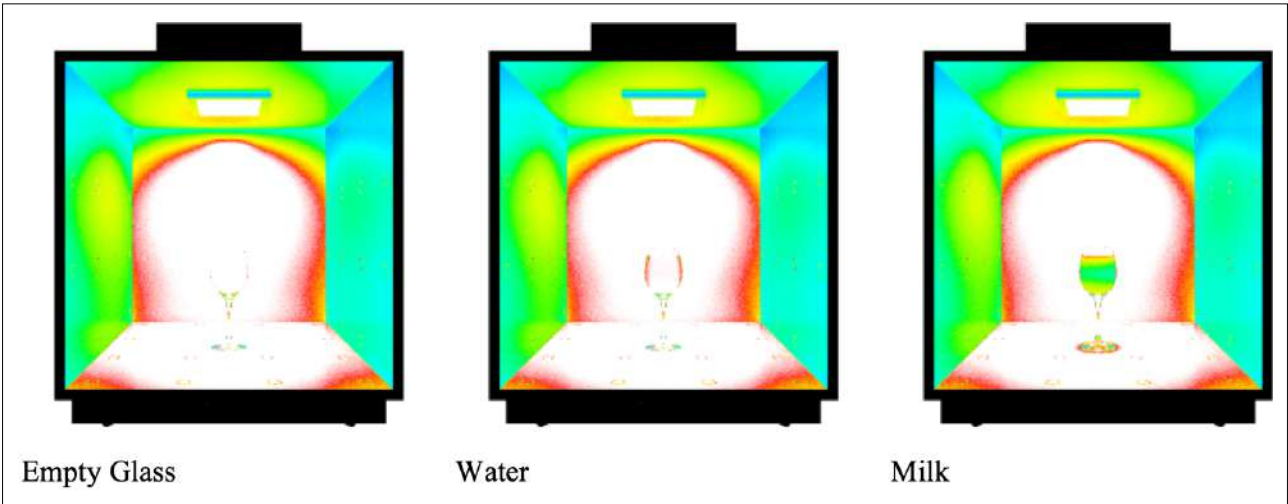


Figure 14. V-ray light analysis renders of empty glass, water, and milk.

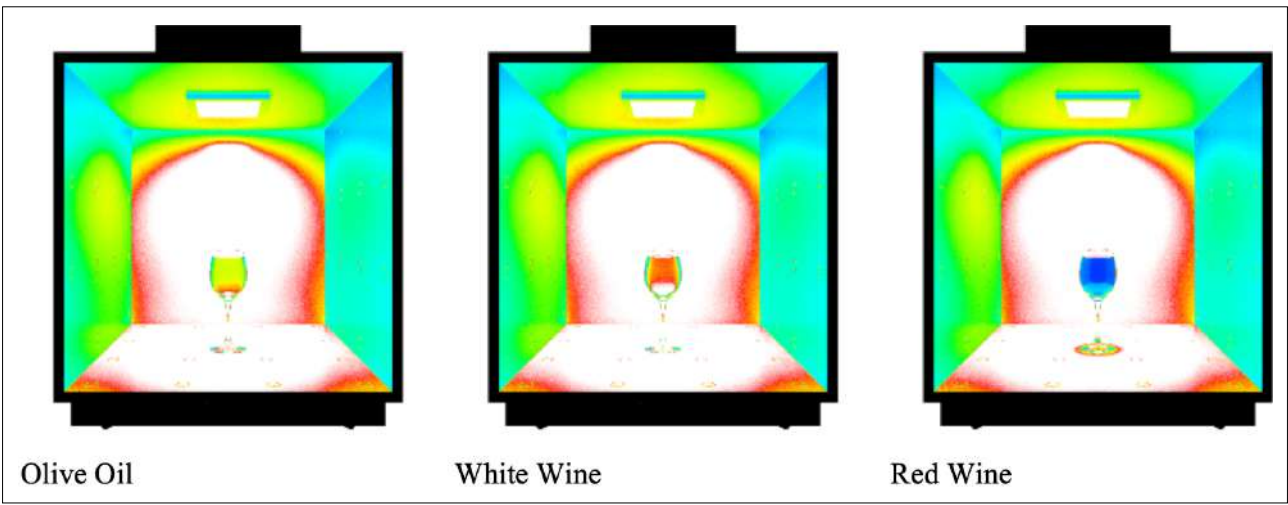


Figure 15. V-ray light analysis renders of olive oil, white wine, and red wine.

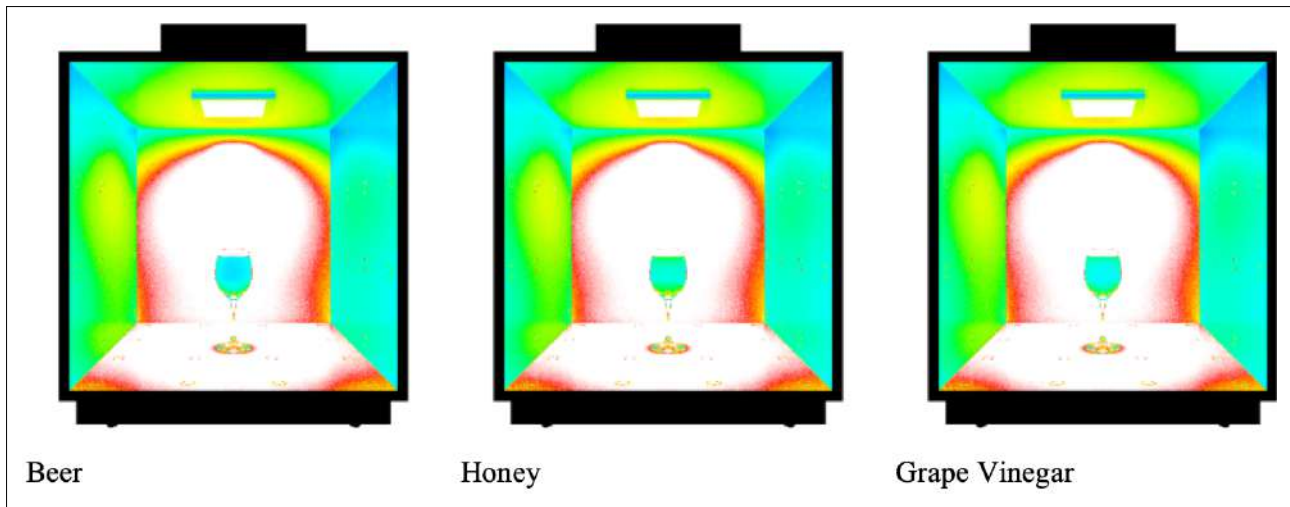


Figure 16. V-ray light analysis renders of beer, honey, and grape vinegar.



Figure 17. Corona realistic renders of empty glass, water, and milk.



Figure 18. Corona realistic renders of olive oil, white wine, and red wine.

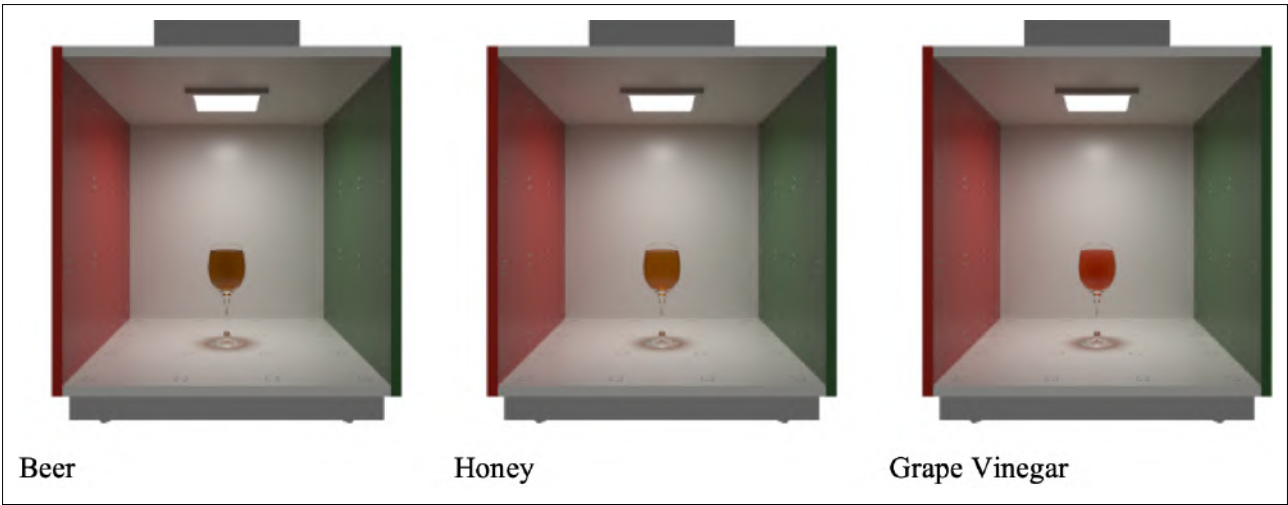


Figure 19. Corona realistic renders of beer, honey, and grape vinegar.

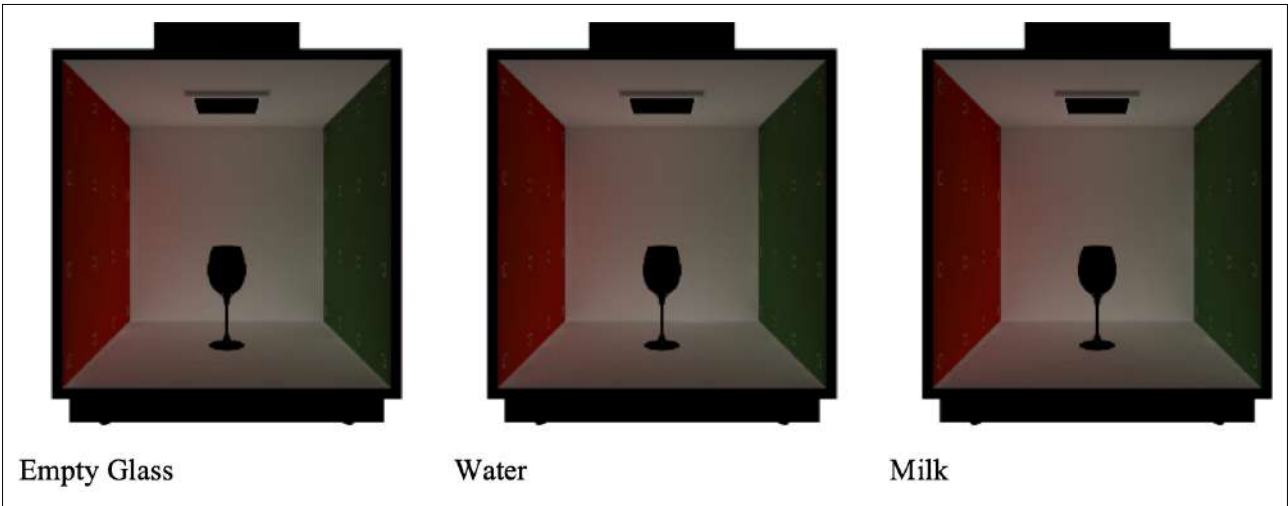


Figure 20. Corona indirect light renders of empty glass, water, and milk.



Figure 21. Corona indirect light renders of olive oil, white wine, and red wine.



Figure 22. Corona indirect light renders of beer, honey, and grape vinegar.

Shader Variables

- **base_color:** A variable of type “color” that represents the base color of the material. Color(1.0, 1.0, 1.0) : Default white color
- **liquid_name:** A variable of type “string” representing the name of the liquid. The user can specify this value in the interface.

string liquid_name = "Custom Liquid";

- **absorption_value:** A “float” variable representing the absorption value of the selected liquid. The user can specify this value in the interface.

float absorption_value = 0.1;

0.1 : Default absorption value

min = 0.0, max = 1.0 : Minimum and maximum values

- **custom_absorption:** A “float” variable representing the absorption value for a user-specified type of liquid.

float custom_absorption = 0.1;

0.1 : Default absorption value

min = 0.0, max = 1.0 : Minimum and maximum values

- **absorption_influence:** A variable of type “float” representing the local absorption effect.

float absorption_influence = 1.0;

1.0 : Default absorption value

- **influence_radius:** A variable of type “float” representing the radius of influence of regional effects. float influence_radius = 1.0;

1.0 : Default radius of influence

- **result:** A variable of type “output color” representing the final calculated color.

output color result = color(0.1, 0.1, 0.1);

- **transform:** A function that performs the transformation of the current point.

point Pobj = transform ("object", P);

"object" : Transform type

"P" = Valid point

- **getattribute:** A function to get the value of the specified attribute.

if (getattribute(("occlusion", dirt_value)) { ... }

"occlusion" : The attribute name to retrieve.

"dirt_value" = Variable to store the value in.

The OSL code prepared according to the variables explained above is connected to the diffuse channel of the base material (Figure 23). Therefore, the light entering the material is defined to affect the environment and itself after being absorbed. In addition, an easy interface is provided to enter data (Figure 24).

Shader Code

shader AbsorptionProximity(

color base_color = color(1.0, 1.0, 1.0), // Base color of the material

int liquid_type = 0 // Type of liquid

[[string widget = "mapper",

string options = "Water:0| Milk:1| Beer:2| OliveOil:3| Honey:4| GrapeVinegar:5| WhiteWine:6| RedWine:7| Other:8",

string label = "Liquid Type",

string description = "Select the type of liquid for absorption properties"]],

float custom_absorption = 0.1 // Custom absorption value for "Other" liquid type



Figure 24. OSL code interface.

```
[[ string label = "Custom Absorption",
    string description = "Custom absorption value for
'Other' liquid type",
    float min = 0.0, float max = 1.0, string visible_when =
"liquid_type == 8" ]],
    output float absorption_value = 0.1 // Absorption value
for the selected liquid
    [[ string label = "Absorption Value",
        string description = "Absorption value for the selected
liquid",
        float min = 0.0, float max = 1.0, string visible_when =
"liquid_type != 8" ]],
        float absorption_influence = 1.0, // Influence factor for
surrounding absorption
        float influence_radius = 1.0, // Radius of influence for
surrounding objects
        output color result = color(1.0, 1.0, 1.0) // Output color
    )
    {
        // Local variable to store the absorption value based on
the selected liquid type
        float base_absorption;
        // Set the base_absorption based on the selected liquid
type
        if (liquid_type == 0) {
            base_absorption = 0.1; // Water
```

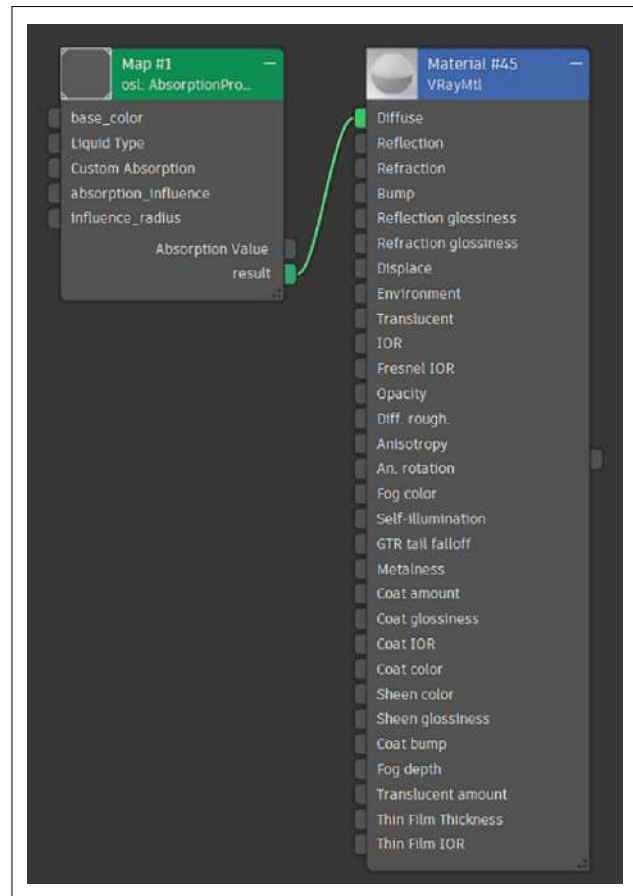


Figure 23. OSL shading network.

```
} else if (liquid_type == 1) {
    base_absorption = 0.5; // Milk
} else if (liquid_type == 2) {
    base_absorption = 0.3; // Beer
} else if (liquid_type == 3) {
    base_absorption = 0.7; // Olive Oil
} else if (liquid_type == 4) {
    base_absorption = 0.8; // Honey
} else if (liquid_type == 5) {
    base_absorption = 0.6; // Grape Vinegar
} else if (liquid_type == 6) {
    base_absorption = 0.2; // White Wine
} else if (liquid_type == 7) {
    base_absorption = 0.4; // Red Wine
} else if (liquid_type == 8) {
    base_absorption = custom_absorption; // Custom value
for Other
}
```

```

// If the selected liquid is not "Other", update the
absorption_value for the UI
if (liquid_type != 8) {
    absorption_value = base_absorption;
}
// Get the current point in object space
point Pobj = transform("object", P);
// Calculate a simple dirt value based on proximity
float dirt_value = 0.0;
if (getattribute("occlusion", dirt_value)) {
    // Calculate adjusted absorption value
    float adjusted_absorption = base_absorption;
    if (dirt_value > 0.0) {
        float influence_factor = 1.0 - dirt_value;
        adjusted_absorption += influence_factor * absorption_
influence;
    }
    // Calculate the final color based on absorption
    result = base_color * (1.0 - adjusted_absorption);
} else {
    result = base_color;
}
}

```

CONCLUSION

In the Cornell box experiment, as a result of precise measurements, the luminance values on the box surfaces were different for each different liquid. The luminance value on the box surface is the sum of direct and indirect light energy. Indirect light energy is affected by light reflected from surfaces and absorbed and scattered within the liquid. The difference in the measurements here is due to the different absorption and scattering values of each liquid. However, in the experiment with realistic image processing software, the results on the Cornell box surfaces are almost identical. The reason for this is that there is no absorption parameter in the material definitions in the software. From a physical perspective, in the real world, all materials except dielectric materials have a light absorption rate. The missing parameters in the liquid materials were added with the Open Shading Language, and an experimental study was put forward. Open Shading Language is an open-source software and has been preferred because it has support for many software. Different software languages can also be preferred instead. The important factor here is to be aware of the absorption parameter. This work continues to be developed.

As a result, it is necessary to use participating media models together with BRDF illumination models in realistic image processing software. Using participating media means that absorption and scattering coefficients are included in the calculations. Thus, the light energy that bounces off objects and incidents on surfaces in global illumination can be more accurately described. In addition, a pre-measured preliminary absorption and scattering value of each liquid can be defined. This method will reduce the computational cost as in the Data-Driven BRDF model. This approach will contribute to more accurate results in all areas of realistic image synthesis. In addition to realistic image synthesis, surface and volume calculation image processing algorithms will also be necessary in areas such as building information modeling, structural physics, and material analysis. Finally, the absorption coefficient must be taken into account in all simulation models related to light.

ETHICS: There are no ethical issues with the publication of this manuscript.

PEER-REVIEW: Externally peer-reviewed.

CONFLICT OF INTEREST: The authors declared no potential conflicts of interest with respect to the research, authorship, and/or publication of this article.

FINANCIAL DISCLOSURE: The authors declared that this study has received no financial support.

REFERENCES

- Akenine-Möller, T., Haines, E., Hoffman, N., Pesce, A., Iwanicki, M., & Hillaire, S. (2018). *Real-Time Rendering, Fourth Edition*. CRC Press. <https://doi.org/10.1201/b22086>
- Angel, E., & Shreiner, D. (2020). *Interactive Computer Graphics: A Top-Down Approach with WebGL, Eighth Edition*. Pearson.
- Ashikhmin, M., & Shirley, P. (2000). An anisotropic phong BRDF model. *Journal of Graphics Tools*, 5(2), 25–32. <https://doi.org/10.1080/10867651.2000.10487522>
- Blinn, J. F. (1977). Models of light reflection for computer synthesized pictures. *ACM SIGGRAPH Computer Graphics*, 11(2), 192–198. <https://doi.org/10.1145/965141.563893>
- Cerezo, E., Pérez, F., Pueyo, X., Seron, F. J., & Sillion, F. X. (2005). A survey on participating media rendering techniques. *The Visual Computer*, 21(5), 303–328. <https://doi.org/10.1007/s00371-005-0287-1>
- Cohen, M. F., & Wallace, J. W. (1993). *Radiosity and Realistic Image Synthesis*. Academic Press.
- Cook, R. L., & Torrance, K. E. (1981). A reflectance model for computer graphics. *ACM Transactions on Graphics (TOG)*, 1(1), 7–24. <https://doi.org/10.1145/357290.357293>

- Deng, H., Wang, B., Wang, R., & Holzschuch, N. (2020). A practical path guiding method for participating media. *Computation Visual Media*, 6(1), 37–51. <https://doi.org/10.1007/s41095-020-0160-1>
- Dür, A. (2006). An improved normalization for the ward reflectance model. *Journal of Graphics Tools*, 11(1), 51–59. <https://doi.org/10.1080/2151237X.2006.10129215>
- Dutr  , P., Bala, K., & Bekaert, P. (2006). *Advanced Global Illumination, Second Edition*. A K Peters. <https://doi.org/10.1201/b10632>
- Geisler-Moroder, D., & D  r, A. (2010). A new ward BRDF model with bounded Albedo. *Computer Graphics Forum*, 29(4), 1391–1398. <https://doi.org/10.1111/j.1467-8659.2010.01735.x>
- Goral, C. M., Torrance, K. E., Greenberg, D. P., & Battaille, B. (1984). Modeling the interaction of light between diffuse surfaces. *ACM SIGGRAPH Computer Graphics*, 18(3), 213–222. <https://doi.org/10.1145/964965.808601>
- Guarnera, D., Guarnera, G. C., Ghosh, A., Denk, C., & Glencross, M. (2016). BRDF representation and acquisition. *Computer Graphics Forum*, 35(2), 625–650. <https://doi.org/10.1111/cgf.12867>
- He, X. D., Torrance, K. E., Sillion, F. X., & Greenberg, D. P. (1991). A comprehensive physical model for light reflection. *ACM SIGGRAPH Computer Graphics*, 25(4), 175–186. <https://doi.org/10.1145/127719.122738>
- Herholz, S., Zhao, Y., Elek, O., Nowrouzezahrai, D., Lensch, H. P. A., & Kr  iv  nek, J. (2019). Volume path guiding based on zero-variance random walk theory. *ACM Transactions on Graphics (TOG)*, 38(3), 1–19. <https://doi.org/10.1145/3230635>
- Jensen, H. W. (2001). *Realistic Image Synthesis Using Photon Mapping*. A K Peters. <https://doi.org/10.1201/b10685>
- J  nsson, D., Sund  n, E., Ynnerman, A., & Ropinski, T. (2014). A survey of volumetric illumination techniques for interactive volume rendering. *Computer Graphics Forum*, 33(1), 27–51. <https://doi.org/10.1111/cgf.12252>
- Kajiya, J. T. (1986). The rendering equation. *ACM SIGGRAPH Computer Graphics*, 20(4), 143–150. <https://doi.org/10.1145/15886.15902>
- Kr  iv  nek, J., Georgiev, I., Hachisuka, T., V  voda, P.,   ik, M., Nowrouzezahrai, D., & Jarosz, W. (2014). Unifying points, beams, and paths in volumetric light transport simulation. *ACM Transactions on Graphics (TOG)*, 33(4), 1–13. <https://doi.org/10.1145/2601097.2601219>
- Kurachi, N. (2007). *The Magic of Computer Graphics*. CRC Press.
- Matusik, W., Pfister, H., Brand, M., & McMillan, L. (2003). A data-driven reflectance model. *ACM Transactions on Graphics (TOG)*, 22(3), 759–769. <https://doi.org/10.1145/882262.882343>
- Neumann, L., Neumann, A., & Szirmay-Kalos, L. (1999). Compact metallic reflectance models. *Computer Graphics Forum*, 18(3), 161–172. <https://doi.org/10.1111/1467-8659.00337>
- Nov  k, J., Georgiev, I., Hanika, J., & Jarosz, W. (2018). Monte Carlo methods for volumetric light transport simulation. *Computer Graphics Forum*, 37(2), 551–576. <https://doi.org/10.1111/cgf.13383>
- Nov  k, J., Nowrouzezahrai, D., Dachsbacher, C., & Jarosz, W. (2012). Virtual ray lights for rendering scenes with participating media. *ACM Transactions on Graphics (TOG)*, 31(4), 1–11. <https://doi.org/10.1145/2185520.2185556>
- Oren, M., & Nayar, S. K. (1994). Generalization of Lambert's reflectance model. *SIGGRAPH '94: Proceedings of the 21st annual conference on Computer graphics and interactive techniques*, 239–246. <https://doi.org/10.1145/192161.192213>
- Peddie, J. (2019). *Ray Tracing: A Tool for All*. Springer. <https://doi.org/10.1007/978-3-030-17490-3>
- Phong, B. T. (1975). Illumination for computer generated pictures. *ACM Communications of the ACM*, 18(6), 311–317. <https://doi.org/10.1145/360825.360839>
- Schlick, C. (1994). An Inexpensive BRDF Model for Physically-based Rendering. *Computer Graphics Forum*, 13(3), 233–246. <https://doi.org/10.1111/1467-8659.1330233>
- Siegel, R., & Howell, J. R. (1992). *Thermal Radiation Heat Transfer, Third Edition*. Taylor & Francis.
- Torrance, K. E., & Sparrow, E. M. (1967). Theory for off-specular reflection from roughened surfaces. *Journal of the Optical Society of America*, 57(9), 1105–1114. <https://doi.org/10.1364/JOSA.57.001105>
- Wang, B., & Holzschuch, N. (2017). Point-based rendering for homogeneous participating media with refractive boundaries. *IEEE Transactions on Visualization and Computer Graphics*, 24(10), 2743–2757. <https://doi.org/10.1109/TVCG.2017.2768525>
- Ward, G. J. (1992). Measuring and modeling anisotropic reflection. *ACM Communications of the ACM*, 26(2), 265–272. <https://doi.org/10.1145/142920.134078>
- Whitted, T. (1980). An improved illumination model for shaded display. *ACM Communications of the ACM*, 23(6), 343–349. <https://doi.org/10.1145/358876.358882>
- Yan, LQ., Zhou, Y., Xu, K., & Wang, R. (2013). Accurate translucent material rendering under spherical Gaussian lights. *Computer Graphics Forum*, 31(7), 2267–2276. <https://doi.org/10.1111/j.1467-8659.2012.03220.x>
- Zhou, Y. (2023). An overview of BRDF models in computer graphics. *Theoretical and Natural Science*, 19, 205–210. <https://doi.org/10.54254/2753-8818/19/20230550>